

# Satellite observations of atmospheric SO<sub>2</sub> from volcanic eruptions during the time-period of 1996–2002

M.F. Khokhar<sup>a,\*</sup>, C. Frankenberg<sup>a</sup>, M. Van Roozendael<sup>b</sup>, S. Beirle<sup>a</sup>,  
S. Kühl<sup>a</sup>, A. Richter<sup>c</sup>, U. Platt<sup>a</sup>, T. Wagner<sup>a,1</sup>

<sup>a</sup> Institute of Environmental Physics, DOAS Satellite group, University of Heidelberg, INF 229, 69120 Heidelberg, BW, Germany

<sup>b</sup> Belgian Institute for Space Aeronomy (IASB-BIRA), Brussels, Belgium

<sup>c</sup> Institute of Environmental Physics, University of Bremen, Bremen, Germany

Received 1 November 2004; received in revised form 24 April 2005; accepted 27 April 2005

## Abstract

In this article, we present satellite observations of atmospheric sulfur dioxide (SO<sub>2</sub>) from volcanic eruptions. Global ozone monitoring experiment (GOME) data for the years 1996–2002 is analyzed using a DOAS based algorithm with the aim of retrieving SO<sub>2</sub> slant column densities (SCD). The retrieval of SO<sub>2</sub> SCD in the UV spectral region is difficult due to strong and interfering ozone absorptions. It is also likely affected by instrumental effects. We investigated these effects in detail to obviate systematic biases in the SO<sub>2</sub> retrieval. A quantitative study of about 20 volcanoes from Italy, Iceland, Congo/Zaire, Ecuador, Japan, Vanuatu Island and Mexico is presented. The focus is on both eruption and out gassing scenarios. We prepared a 7-year mean map (1996–2002) of SO<sub>2</sub> SCD observed by GOME and tabulated the ratios of the maximum SO<sub>2</sub> SCD observed to the average SO<sub>2</sub> SCD as seen in the 7-year mean map. The further aim of this study is to provide information about unknown volcanic eruptions, e.g., Bandai Honshu Japan, Central Islands Vanuatu, Piton de la Fournaise Réunion Island France, Kamchatka region of Russia and from Indonesia especially. The results demonstrate a high sensitivity of the GOME instrument towards SO<sub>2</sub> emissions during both eruption and degassing episodes.

© 2005 COSPAR. Published by Elsevier Ltd. All rights reserved.

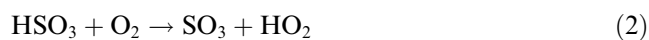
**Keywords:** Satellite remote sensing; GOME; SO<sub>2</sub> SCD; Volcanic eruptions; Out gassing; ratio

## 1. Introduction

Sulfur dioxide (SO<sub>2</sub>) is an important trace species in the atmosphere, both under background conditions and in polluted areas. It is released to the troposphere as a result of anthropogenic and natural phenomena.

In the presence of clouds, SO<sub>2</sub> is rapidly taken up into the liquid phase and converted to H<sub>2</sub>SO<sub>4</sub> leading to a lifetime of SO<sub>2</sub> of only a few hours. In the absence of

clouds, the conversion into H<sub>2</sub>SO<sub>4</sub> takes place via the gas phase (Eqs. (1)–(3)) resulting in a much longer lifetime of about several days (Eisinger and Burrows, 1998; von Glasow et al., 2002). In the dry stratosphere, particularly in the lower stratosphere where the concentration of OH is relatively small, the lifetime of SO<sub>2</sub> is longer than in the troposphere being of the order of several weeks (Eisinger and Burrows, 1998):



\* Corresponding author. Tel.: +49 6221 545477; fax: +49 6221 546405.

E-mail addresses: [mfkhokhar@iup.uni-heidelberg.de](mailto:mfkhokhar@iup.uni-heidelberg.de) (M.F. Khokhar), [thomas.wagner@iup.uni-heidelberg.de](mailto:thomas.wagner@iup.uni-heidelberg.de) (T. Wagner).

<sup>1</sup> Tel.: +49 6221 546314; fax: +49 6221 546405.

Volcanoes are an important natural source of various atmospheric trace gases. Volcanic eruptions inject gases and particles into the atmosphere, leading to stratospheric and tropospheric aerosol formation. Highly explosive volcanic events, like Pinatubo in 1991, affect the climate on time scales of months to years (McCormick et al., 1995). Therefore, the quantification of the magnitude and variability of volcanic SO<sub>2</sub> output plays an important role in assessing the natural radiative forcing of atmospheric sulfate aerosols. Since volcanic eruptions and their emissions are sporadic and intermittent and often occur in uninhabited regions, assessing the amount and size of the gaseous and particulate emission from volcanoes is difficult. Satellite remote sensing measurements provide one well-suited opportunity to overcome this difficulty (Krueger et al., 1995; Afe et al., 2004).

From global ozone monitoring experiment (GOME) observations we analyse the total atmospheric vertical column density (VCD), that is the integrated SO<sub>2</sub> concentration (for details, see Section 2.2). This quantity is proportional to the total emissions of SO<sub>2</sub>:

$$E = \text{VCD}/\tau. \quad (4)$$

Here,  $\tau$  is the atmospheric lifetime of SO<sub>2</sub> and  $E$  is the SO<sub>2</sub> emission in units of molecules/cm<sup>2</sup> per day. For an atmospheric lifetime of 1 day, the SO<sub>2</sub> VCD equals the SO<sub>2</sub> emission per day. Since the atmospheric lifetime of SO<sub>2</sub> is typically of the order of a few days, the daily SO<sub>2</sub> emissions are in general smaller than the measured SO<sub>2</sub> VCD. We present GOME data analyzed for the period January 1996–December 2002.

It should be noted that in reality, the atmospheric lifetime is highly variable, depending in particular on altitude of the SO<sub>2</sub> plume and the presence of clouds. In addition, SO<sub>2</sub> emissions especially from volcanoes are often not continuous. Further complications might arise from the coarse sampling of GOME (see Section 2.1). Thus, our simple picture (Eq. (4)) can only yield a rough estimate of the emissions.

## 2. GOME instrument and data analysis

### 2.1. Global ozone monitoring experiment

GOME is a nadir-scanning ultraviolet and visible spectrometer for global monitoring of atmospheric ozone covering the wavelength range from 240 to 790 nm (Burrows et al., 1999). It was launched on-board ERS-2 in April 1995 into a near-polar Sun synchronous orbit at a mean altitude of 790 km with a local equator crossing time at 10:30 am. Total ground coverage is obtained within 3 days at the equator by a 960 km across-track swath. For the measurements presented in this work, the ground pixel size is 40 (along track) \* 320

(across track) km<sup>2</sup>. A key feature of GOME is its ability to detect, besides ozone, several chemically active atmospheric trace gases such as SO<sub>2</sub>, NO<sub>2</sub>, BrO, H<sub>2</sub>O, OClO and CH<sub>2</sub>O.

### 2.2. Data analysis

GOME measures the direct solar spectrum (irradiance) and the Earthshine radiance, i.e., the sunlight reflected by earth's surface or scattered back by molecules and aerosols in the atmosphere. From the ratio of earthshine radiance and solar irradiance measurements (level 1 version 1.3), slant column densities (SCD) of the respective absorbers can be derived by applying the technique of differential optical absorption spectroscopy (DOAS) (Perner and Platt, 1979; Platt, 1994; Richter et al., 1998; Wagner et al., 2001a,b). The SCD is the integrated concentration along the effective light path. For the conversion of the measured SO<sub>2</sub> SCD into the vertical column density (VCD) an air mass factor (AMF) is applied, which is defined as the ratio of the SCD and the VCD:

$$\text{VCD} = \text{SCD}/\text{AMF}. \quad (5)$$

The calculation of appropriate SO<sub>2</sub>-AMFs is complicated by several factors. First the SO<sub>2</sub>-AMF depends strongly on the SO<sub>2</sub> profile, which largely differs for the different types of sources. Furthermore, it also strongly depends on the surface albedo, clouds and aerosols loading (Thomas et al., 2005). Information about all these parameters is usually not available for a given GOME SO<sub>2</sub> analysis. From our sensitivity studies (see Fig. 1), we found that for all scenarios the SO<sub>2</sub>-AMF shows only a weak SZA dependence for SZA < 80°. Therefore, we decided to apply an average AMF of unity for this study, which means that the SO<sub>2</sub> VCD equals the retrieved SCD. This approximation fits in particular to the following average observation properties: surface albedo: 3%, (no snow and ice on the ground); aerosol optical depth: 0.1; cloud fraction: 20% (clouds are assumed to be above the SO<sub>2</sub> plume); height of the SO<sub>2</sub> plume: 4–5 km. While these assumptions might well describe typical volcanic plumes, for individual situations also large differences can occur. Appropriate correction factors are given in Table 1.

SO<sub>2</sub> exhibits relatively weak absorptions in the UV and a wavelength window between 312.5 and 327.6 nm is used for the retrieval. In this spectral region, the strong ozone Huggins band overlaps the weak SO<sub>2</sub> absorptions. Thus, a precise knowledge of the instrumental function, which convolves the incoming highly structured signal to instrumental resolution, is indispensable, since small uncertainties in the spectral structure of strong absorbers can result in residuals that are larger than the weak SO<sub>2</sub> absorption itself. Narrow Fraunhofer lines are well suited to derive information on the

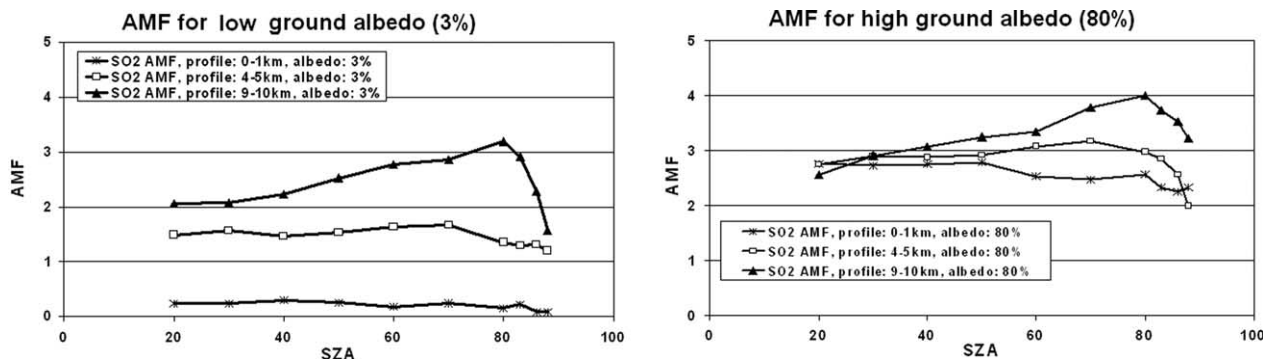


Fig. 1. SO<sub>2</sub>-AMFs calculated for different scenarios (without clouds). While the AMFs only weakly depend on the SZA, they show a strong dependence on the ground albedo. The AMFs were calculated with the Monte-Carlo radiative transfer model TRACY (Hönninger et al., 2004; von Friedeburg, 2003). The scatter of the data is due to limited statistics and can be reduced if a higher number of photons are modeled.

Table 1  
Correction factors for the standard GOME SO<sub>2</sub> VCD for specific scenarios

Scenario (altitude of SO <sub>2</sub> plume) (km)	No clouds	50% Cloud fraction (clouds below SO <sub>2</sub> )	50% Cloud fraction (clouds above SO <sub>2</sub> )
0–1	3.3	0.5	10
4–5	0.66	0.4	2
9–10	0.3–0.5	0.25–0.4	0.6–1

The standard VCD have to be multiplied by these factors.

instrumental function. Based on the work of Van Roozendaal et al. (2002), we applied a nonlinear least squares fit to find an optimum slit function by fitting a highly resolved solar spectrum (Kurucz et al., 1984; Chance and Spurr, 1997) to the solar irradiance measurement of GOME. The slit function could be approximated by an asymmetric Voigt line shape.

Furthermore, the width and asymmetry are strongly wavelength dependent. We used this asymmetric and wavelength dependent slit function to convolve the highly resolved laboratory spectra of SO<sub>2</sub>, two Ozone spectra at different temperatures (both deconvoluted

using the known SCIAMACHY line shape) and the Ring spectrum, thereby creating an optimal set of reference spectra (Table 2) at instrumental resolution at instrumental resolution. Nevertheless, in the analyzed data sets of SO<sub>2</sub> we still find a latitudinal dependent bias, which is probably caused by a remaining spectral interference with an imperfect “removal” of the strong O<sub>3</sub> absorptions. The atmospheric O<sub>3</sub> absorption increases strongly and systematically towards polar latitudes because of the increase of the solar zenith angle. The retrieval of SO<sub>2</sub> column densities in the UV wavelength region is also strongly affected by the spectral interference due to diffuser plate structures (Richter and Wagner, 2001). These are artificial spectral structures induced by the diffuser plate which is used for solar irradiance measurements.

These structures vary with the position of the sun, leading to a seasonally varying offset in SO<sub>2</sub>, which does not depend on latitude. Apart from these complications, which result in a constant and a latitudinal varying offset in the retrieved SO<sub>2</sub> SCDs, we found systematically enhanced columns over high and bright surfaces (Fig. 2(a)).

Although, we cannot completely rule out real local enhancements of the SO<sub>2</sub> concentrations, these findings

Table 2  
Reference spectra used for SO<sub>2</sub> columns retrieval from GOME data

Spectra	Specification	Reference/source
O <sub>3</sub> <sup>a</sup>	Temperature: 223 K, vacuum, deconvoluted	Bogumil et al. (2003) <a href="http://www.iup.physik.uni-bremen.de/gruppen/molspec/SCIA.html">http://www.iup.physik.uni-bremen.de/gruppen/molspec/SCIA.html</a>
O <sub>3</sub> <sup>b</sup>	Temperature: 243 K, vacuum, deconvoluted	Bogumil et al. (2003) <a href="http://www.iup.physik.uni-bremen.de/gruppen/molspec/SCIA.html">http://www.iup.physik.uni-bremen.de/gruppen/molspec/SCIA.html</a>
SO <sub>2</sub>	Temperature: 273 K, vacuum	Bogumil et al. (2003) <a href="http://www.iup.physik.uni-bremen.de/gruppen/molspec/SCIA.html">http://www.iup.physik.uni-bremen.de/gruppen/molspec/SCIA.html</a>
Solar	Solar irradiance	Measured by GOME on 01-06-1997 used as fixed solar reference
Ring	Calculated from solar spectrum	Bussemer (1993)
Ratio	See Section 2.2	Measured by GOME, see Section 2.2

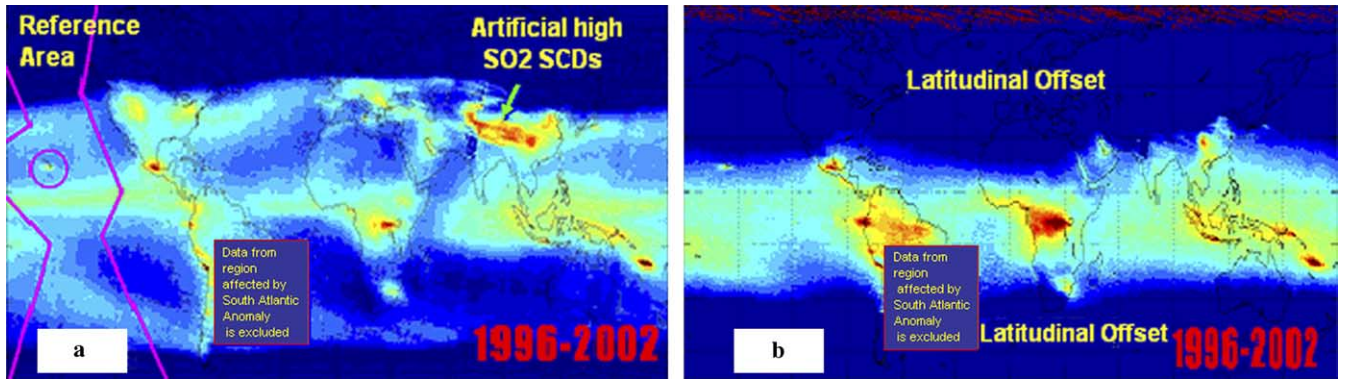


Fig. 2. Global map of SO<sub>2</sub> SCD averaged over 7 years. In (a), the results of the original DOAS fit are displayed. Besides a constant offset and a latitudinal varying offset also enhanced SO<sub>2</sub> SCD are found over bright surfaces. Including an additional ratio spectrum in the DOAS analysis (see text) nearly completely removes these enhanced values (b). The SO<sub>2</sub> offset is removed by subtracting the results from a reference sector (magenta lines).

are very probable related to spectral interferences with an imperfect correction for the Ring effect (Van Roozendael et al., 2002).

In this work, we apply a preliminary and simple method to avoid these artefacts: We include a ratio spectrum, which contains the spectral structures of high and bright surfaces, in the DOAS fit. To this end, we used the ratio of a pixel directly over the Himalaya and a nearby pixel in northern India from GOME orbit 61204045 on 12th of December 1996. Including this ‘correction spectrum’ in the spectral analysis nearly completely removes the enhanced SO<sub>2</sub> values over bright surfaces (Fig. 2(b)).

To correct the constant and latitudinal varying offsets described before, we normalize our retrieved columns by a reference sector method (RSM) (for details see Richter and Burrows (2002) and Martin et al. (2002)). This method uses a presumably SO<sub>2</sub> free reference sector over a remote area (Magenta line on Fig. 2(a), while the circle indicates the Hawaiian Island region excluded from the reference sector), in order to calculate offset values of SO<sub>2</sub> columns at each latitude. In brief, this method applies a correction for each latitude so that the reference sector exhibits a SCD of zero after the correction (Fig. 3). From the residual structures of the spectral DOAS analysis and the homogeneity of the results we estimate

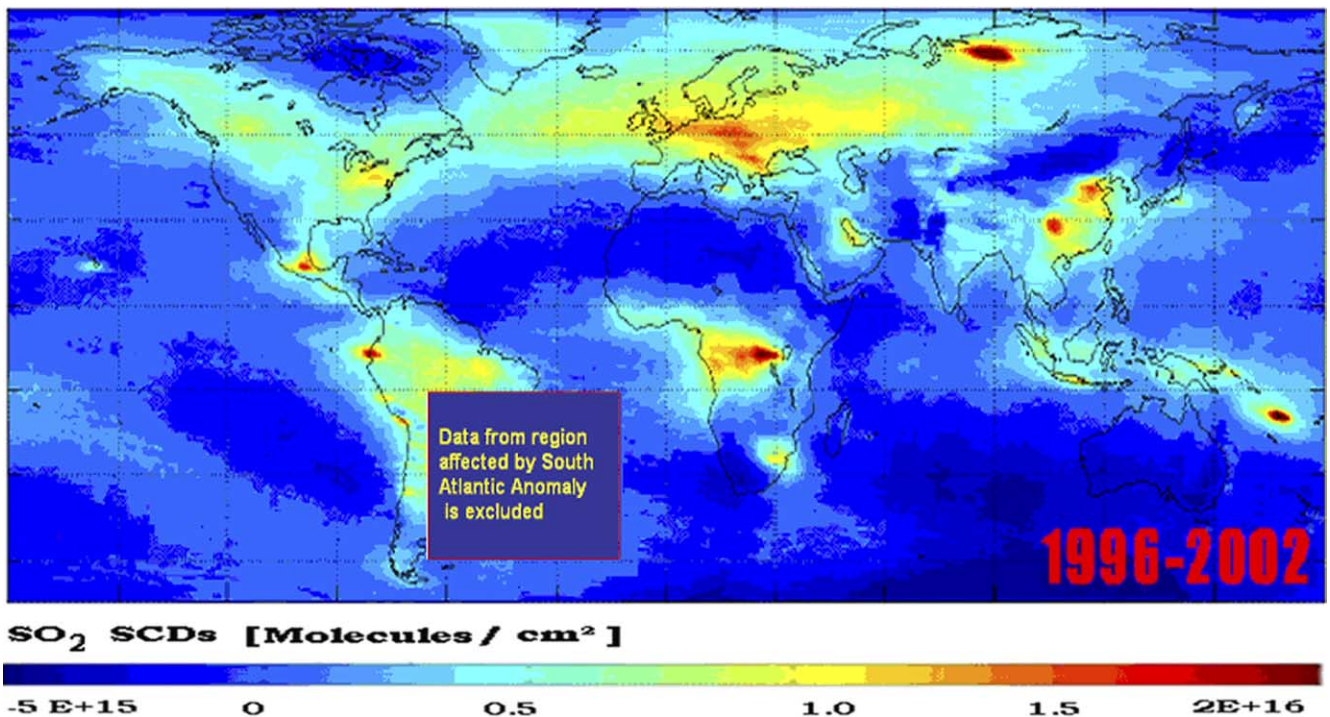


Fig. 3. 7-year mean maps of GOME SO<sub>2</sub> SCD from 1996 to 2002 after all corrections are applied. The GOME observations are averaged on a 0.5° latitude/longitude grid. Note that in a first approximation the measured SO<sub>2</sub> SCD can be considered a good proxy for the SO<sub>2</sub> VCD (see Fig. 1 and related text). For individual observations correction factors listed in Table 1 can be applied.

our detection limit to be about  $2 \times 10^{16}$  molecules/cm<sup>2</sup> for daily maps.

### 3. Results

In this section, we give an overview of SO<sub>2</sub> SCD observed by GOME from different volcanic events. First,

we present a global map averaged over 7 years from 1996 to 2002 (Fig. 3). In addition, we present an overview on several individual eruptions of various volcanoes (Fig. 4). It is interesting to note that according to Eqs. (4) and (5) the SO<sub>2</sub> emissions can be estimated from the measured SO<sub>2</sub> SCD. For an assumed SO<sub>2</sub> lifetime of 1 day and an AMF of 1 (see Fig. 1 and Table 1), the measured SO<sub>2</sub> represents the daily SO<sub>2</sub> emissions. It

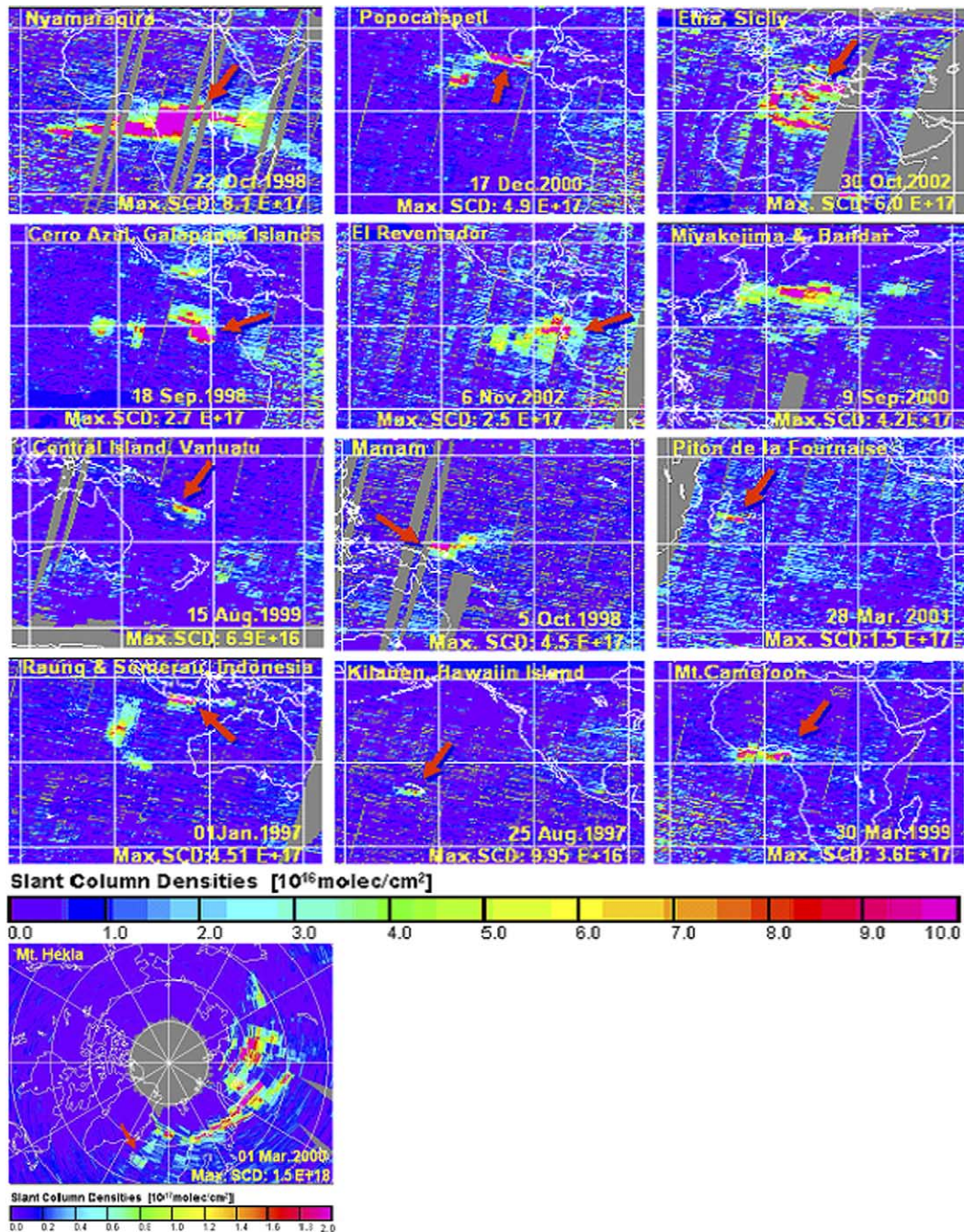


Fig. 4. 3-day mean maps of SO<sub>2</sub> SCD for different volcanoes during events with maximum observed SO<sub>2</sub> SCD from 1996 to 2002. The GOME observations are averaged on a 0.5° latitude/longitude grid. The name of the volcano and the maximum SO<sub>2</sub> SCD is included in the maps. The Red arrow pointing to the position of each volcano as indicated by name on each map. More information on the presented examples is given in Table 2. Please note that the color scale is different for the Hekla eruption.

should be again noted that Eq. (4) can only yield a rough estimate of the emissions (see comments at the end of Section 1).

Fig. 3 illustrates that GOME data holds plenty of information on the different SO<sub>2</sub> sources including both anthropogenic and natural. For instance the eastern parts of the US, Eastern Europe, “Highveld” region of South Africa, Arabian Gulf, China and particularly the Norilsk region of Russia reveal clearly enhanced levels of SO<sub>2</sub> SCD due to coal power plants, metal ores smelting industry and higher rate of fossil fuel consumptions in these regions. Volcanic eruptions are main natural sources of SO<sub>2</sub> contributions (e.g., from central Africa, Europe, Indonesia, Japan, Vanuatu Island, Ecuador and Mexico, etc.), in addition to Biomass burning particularly from Indonesia, central Africa and Amazon basin of South American continent. No evidence of SO<sub>2</sub> emission from other sources like oxidation of organic matter over ocean and wet lands has been identified from satellite data.

In Fig. 4, we present an overview on major eruptions of 20 volcanoes during the period 1996–2002. We classify an eruption as ‘major eruption’ if the SO<sub>2</sub> SCD is  $>3 \times 10^{16}$  molecules/cm<sup>2</sup> and lasts for more than one day; for  $2 \times 10^{16}$  molecules/cm<sup>2</sup>  $<$  SO<sub>2</sub> SCD  $<$   $3 \times 10^{16}$  molecules/cm<sup>2</sup> we regard a volcano to be in a degassing state. More details on the selected volcanoes and on the measured emissions are given in Table 3. It also includes a comparison with simultaneous TOMS SO<sub>2</sub> observations. We estimated the distance the SO<sub>2</sub> plume propagated during each volcanic event depicted in Fig. 4 by simply setting a lower threshold of  $2.0 \times 10^{16}$  molecules/cm<sup>2</sup>. These calculated values can of course only be a rough measure of the plume extension and depend in particular on the magnitude and duration of the volcanic eruption, atmospheric dynamics and meteorological conditions of that particular region.

Before we discuss some selected case studies in more detail, we briefly discuss some general findings presented in Fig. 4 and Table 3. We calculated the ratios of the maximum SO<sub>2</sub> SCD ever observed during the period 1996–2002 to the average SO<sub>2</sub> SCD as seen from 7-years mean map for each volcano. This ratio can be used for a rough characterization of the type and activity of a volcano. It is in particular strongly dependent on the magnitude, degassing state and other background emissions from the surroundings of each volcanic event. According to the results from Table 2, we can categorize the different volcanoes into three classes with relatively high ratio ( $\geq 40$ ), moderate ratio ( $\geq 25$ ) and low ratio ( $< 25$ ). We find that this ratio is high when there is no or very seldom out gassing like for, e.g., Nyamuragira, Cerro Azul, Piton de la Fournaise, Mt. Cameroon, Hekla, Egmont (with the exception of Mount Etna, Sicily with frequent degassing but smaller number of major eruptions). The ratio is mod-

erate when there is frequent degassing, e.g., Manam & Ulawun Rabul and Miyakejima & Bandai Honshu (with the exceptions from Semeru or Raung and Popocatepetl where the SO<sub>2</sub> emissions from degassing cannot be differentiated from the background SO<sub>2</sub> emission by biomass burning and fossil fuel consumption, respectively). Finally, the ratio is low when the degassing is continuous like, e.g., for Kilauea, El Reventador & Tungurahua, Kamchatka region and Vanuatu volcanic Island.

We found that three of four shield volcanoes studied have high ratio values; the ratios of the strato volcanoes cover all categories equally. We compared our observations to the simultaneously measured SO<sub>2</sub> data from TOMS. We find that for most observations the TOMS SO<sub>2</sub> data are systematically larger compared to the GOME SO<sub>2</sub> SCD.

This is probably caused by the much smaller pixel size of the TOMS observations ( $39 \text{ km} \times 39 \text{ km}$ ) (NASA Earth Science Missions) compared to  $40 \text{ km} \times 320 \text{ km}$  for GOME. In addition, we found that for some cases no enhanced SO<sub>2</sub> values were found by TOMS whereas GOME data showed enhanced SO<sub>2</sub> SCD.

Similarly, TOMS did not observe several other major volcanic eruptions during the time-period from 1996 to 2002. (There could possibly be data gaps for one or two events but this cannot be the case for each event mentioned in Table 2, particularly eruptions from Etna Sicily, Piton de la Fournaise Réunion Island, France, Egmont & Rraupehu New Zealand, Miyakejima & Bandai Honshu, Kilauea Hawaiian Island and from Central Island Vanuatu). This indicates that because of the higher spectral resolution, the ability of GOME to detect small SO<sub>2</sub> absorptions is significantly better. This conclusion is further supported when considering that besides their higher spatial resolution TOMS observations also achieve global coverage within only one day (compared to three days for GOME). It is interesting to note that very recently published results from thermal IR observations made by the AIRS instrument on EOS/aqua (Carn et al., 2005) find nearly the same SO<sub>2</sub> column densities over Etna/Sicily on October, 30, 2002 as derived from GOME.

In a first case study, we investigated the emissions of the most active volcano from the central African region during the last decade: Nyamuragira, a shield volcano in the Virunga volcano field of Zaire/D.R. Congo. Fig. 4 shows the 3 days mean map (22–25 October 1998) of SO<sub>2</sub> SCDs from the Nyamuragira eruption, which started on 18th October 1998. The maximum SCD of  $8.1 \times 10^{17}$  molecules/cm<sup>2</sup> was observed on 22nd of October 1998. In Fig. 4 two kinds of plumes can be seen, the first streams out to south east of the volcano reaching  $\approx 3500 \text{ km}$  south east of Nyamuragira while after some days the plume streamed towards west extending over a distance of 5500 km within one week. During this

Table 3  
Quantitative overview of different volcanic events observed by GOME during time-period 1996–2002, comparison with TOMS observations

Volcano	Region	Location	Volcanic eruptions observed by GOME from 1996 to 2002		Number of volcanic eruptions observed by TOMS during 1996–2002	Maximum SO <sub>2</sub> SCD observed by GOME [molecules/cm <sup>2</sup> ] (according to Fig. 4) <sup>a</sup>	Maximum SO <sub>2</sub> SCD observed by TOMS [molecules/cm <sup>2</sup> ]	Maximum altitude of the SO <sub>2</sub> plume from Global Volcanism Program (GVP) [km]	SO <sub>2</sub> SCD from 7-year mean map [molecules/cm <sup>2</sup> ]	Ratio: maximum SO <sub>2</sub> SCD to 7-year mean SO <sub>2</sub> SCD [molec/cm <sup>2</sup> ]	Approximately maximum distance the SO <sub>2</sub> plume reached (according to Fig. 4) [km]
			Number of major eruptions	Degassing							
Nyamuragira	Zair/D.R. Congo	1.4°S, 29.2°E	5	Very seldom	5	8.1E + 17	8.06E + 17	18 <sup>b</sup>	2.0E + 16	40.5	5500
Popocatepetl <sup>c</sup>	Mexico	9.02°N, 98.62°W	8	Continuous	5	4.9E + 17	1.07E + 18	8	1.9E + 16	25.79	2700
Etna, Sicily	Italy	37.7°N, 15.0°E	2	Frequent	1	6.0E + 17	8.06E + 17	6.4	1.2E + 16	50	1800
Cerro Azul	Ecuador	0.9°S, 91.42°W	2	–	2	2.7E + 17	8.06E + 17	2.1	0.5E + 16	54	4400
Galápagos Island											
El eventador & Tungurahua	Ecuador	0.07°S, 77.6°W, 1.4°S, 78.4°W	(1 + 2) = 3	Continuous	(1 + 2) = 3	2.5E + 17	6.71E + 17	17	2.0E + 16	12.5	2700
Miyakejima & Bandai Honshu	Japan	34.08°N, 139.5°E, 37.6°N, 140.1°E	(2 + 1) = 3	Frequent	(1 + 0) = 1	4.2E + 17	1.07E + 18	15	1.2E + 16	35	4900
Central Island	Vanuatu	16.0°S, 168.5°E	5	Continuous	0	6.9E + 16	–	2	2.0E + 16	3.45	900
Manam & Ulawun, Rabaul	Papa New Guinea	4.1°S, 145.06°E, 5.0°S, 151.3°E	(2 + 2) = 4	Frequent	(2 + 2) = 4	4.5E + 17	1.07E + 18	3	1.3E + 16	34.62	1600
Piton de la Fournaise	Réunion Island France	21.23°S, 55.71°E	2	–	1	1.5E + 17	8.06E + 17	NI	0.2E + 16	75	1200
Semeru or Raung <sup>c</sup>	Java Indonesia	8.12°S, 112.9°E, 8.13°S, 114.04°E	1	–	0	4.9E + 17	–	NI	1.3E + 16	37.69	2800
Kilauea, Hawaii	USA	19.43°N, 155.3°W	4	Frequent	0	9.95E + 16	–	NI	0.9E + 16	11.05	800
Mount Cameroon <sup>c</sup>	Cameroon	4.203°N, 9.170°E	1	Very seldom	1	3.6E + 17	8.06E + 17	NI	0.8E + 16	45	2300
Bezymianny & shieveluch	Kamchatka Russia	55.98°N, 160.58°E, 55.38°N, 161.19°E	3	Very seldom	3 <sup>d</sup>	7.0E + 16	–	10	0.5E + 16	14	700
Hekla	Iceland	63.98°N, 19.70°W	1	–	1	6.5E + 17, 1.52E + 18 <sup>e</sup>	8.06E + 17	12	0.8E + 16	81.25	8500
Egmont & Raupehu	New Zealand	39.3°S, 174.1°E, 39.28°S, 175.5°E	3	Very seldom	0	8.41E + 17	–	NI	0.3E + 16	280	1400

NI, no information about SO<sub>2</sub> plume's altitude but eruption was stated in GVP.

<sup>a</sup> The maximum SO<sub>2</sub> observed either directly over the volcano or in close temporal and/or spatial relation to the eruption.

<sup>b</sup> Information from a source Carn and Bluth (2003) other than GVP but eruption was stated in GVP.

<sup>c</sup> The regions with SO<sub>2</sub> emissions from sources other than volcanic out gassing, e.g., biomass burning and fossil fuel consumptions, etc.

<sup>d</sup> TOMS instrument detected ash and aerosol clouds from these events but could not detect SO<sub>2</sub> column amounts.

<sup>e</sup> These SCD are observed at a location about 4200 km eastward from the volcano.

event and also several other events (December 1996, October 1998, January–February 2000, February 2001 and July 2002) good agreement with TOMS observations was found.

As a second case study, we discuss a volcanic eruption observed by GOME in January 1997 from Java region of Indonesia, as shown in Fig. 4. The eruption seems to have started on 31st of December 1996 and unfortunately there was no satellite overpass on this day. Also, no additional information about this volcanic eruption is available from any other source nor from the TOMS instrument. The most likely eruption was from either Semeru (8.12°S, 112.9°E) or the Raung (8.125°S, 114.042°E) volcano in the Java region. Both volcanoes are situated in the same GOME pixel and therefore cannot be distinguished. Also biomass burning in this region makes it more difficult to differentiate the volcanic SO<sub>2</sub> especially in the case of degassing. The maximum SCD observed was  $4.5E + 17$  molecules/cm<sup>2</sup> on 1st of January 1997. The plumes firstly streamed out to south-west of the volcano and finally to the south reaching a distance of 2800 km over Indian Ocean (Fig. 4).

As a third case study, we discuss Popocatepetl, a large stratovolcano 70 km southeast of Mexico City. It is the second highest and one of the most active volcanoes in Mexican history. Assessing the total amount of SO<sub>2</sub> emitted by Popocatepetl is difficult since the large population of Mexico City and its industrial facilities lead to a significant anthropogenic contribution to the total SO<sub>2</sub> emissions (Eisinger and Burrows, 1998). The maximum SCD of  $4.9E + 17$  molecules/cm<sup>2</sup> was observed on 17th December 2000 and the SO<sub>2</sub> plume reached a distance of 2700 km south-west of the volcano. GOME observed the volcanic activities during the months of March–April, July–October and December 1996, July 1997, November 1998, December 2000, June 2001, and March 2002, while TOMS only observed 5 out of these 8 major events.

A fourth case study shows measurements for the strong Hekla eruption during February–March 2000.

The very high SO<sub>2</sub> SCD of  $1.5E + 18$  molecules/cm<sup>2</sup> observed for this eruption could be due to the following reasons: good sensitivity of GOME either because the SO<sub>2</sub> plume reached high altitudes or due to high surface albedo of underlying snow (see Table 3). It could also be that the plume of the very strong eruption, which started on 26th of February 2000 and continued until 7th of March 2000 either in periodic or continuous way, reached far distances and mixed up with the local SO<sub>2</sub> plume from Norilsk, Russia. The Nickel smelting industry at Norilsk [69°N, 88°E] is the largest single source of anthropogenic SO<sub>2</sub> emissions (Carn et al., 2004) and appears in the 7-year mean map of SO<sub>2</sub> SCD, exhibiting very high SO<sub>2</sub> abundances.

#### 4. Conclusions

We presented global SO<sub>2</sub> data derived from observations of the satellite instrument GOME using the DOAS method. We applied several improvements to our original algorithm, which allowed us to compensate different instrumental and methodological problems. The retrieved SO<sub>2</sub> SCD demonstrate the high sensitivity of the GOME instrument, especially in comparison with observations by the TOMS instrument.

All these observations demonstrate the capability of the GOME instrument to monitor SO<sub>2</sub> emissions during both, volcanic eruptions and degassing scenarios over a period more than 7 years. In spite of relatively large uncertainties for individual observations, GOME SO<sub>2</sub> measurements already allow to yield rough estimates of the corresponding emissions. The uncertainties can be further reduced if additional information on the plume height, the cloud cover, the aerosol load and the SO<sub>2</sub> lifetime become available.

Volcanic emissions are highly variable in space and time. We quantified the SO<sub>2</sub> emissions of several important volcanoes of the world. We calculated the ratio of highest SO<sub>2</sub> SCD ever observed from 1996 to 2002 for each individual volcano to the mean SO<sub>2</sub> SCD as seen in the 7-year period. For shield volcanoes 3 of 4 have high ratios; the ratios of the strato volcanoes cover all categories equally.

GOME's ability to detect SO<sub>2</sub> emissions particularly during out gassing events at high latitude is outstanding compared to other space borne instruments. GOME measurements provide information on the global distribution of atmospheric SO<sub>2</sub>, which is needed for a more accurate modeling of the global sulfur budget (Graf et al., 1997). While the uncertainties are still high, satellite observations have the particular advantage that they cover the whole earth with almost similar sensitivity. In addition, they cover the entire volcanic plumes in both horizontal and vertical dimensions and thus allow to quantify the total emissions of individual eruptions.

The disadvantage of GOME is the relatively coarse spatial resolution (320 km × 40 km). However, this limitation will be improved by other satellite instruments onboard new or future space missions from ESA and NASA, e.g., SCIAMACHY, OMI or GOME2, which have comparably better spatial resolution. The high spatial resolution will help to monitor, localize and study volcanic SO<sub>2</sub> plumes and to quantify the effects of volcanic eruptions on a finer spatial scale.

#### Acknowledgements

The authors acknowledge the financial support and providing ERS-2, GOME data by DLR (Wessling, Germany) and ESA (Frascati, Italy). We especially



acknowledge the TOMS Volcanic Emission Group for statistics from their website <http://toms.umbc.edu/>. In addition, special thanks to all colleagues for their contribution and tremendous help.

## References

- Afe, O.T., Richter, A., Sierk, B., Wittrock, F., Burrows, J.P. BrO emission from volcanoes – a survey using GOME and SCIAMACHY measurements. *Geophys. Res. Lett.* 31, L24113, doi:10.1029/2004GL020994, 2004.
- Bogumil, K., Orphal, J., Homann, T., Voigt, S., Spietz, P., Fleischmann, O.C., Vogel, A., Hartmann, M., Bovensmann, H., Frerick, J., Burrows, J.P. Measurements of molecular absorption spectra with the SCIAMACHY Pre-Flight Model: instrument characterization and reference data for atmospheric remote-sensing in the 230–2380 nm region. *J. Photochem. Photobiol. A: Chem.* 157 (2–3), 167–184, 2003.
- Burrows, J.P., Weber, M., Buchwitz, M., Rozanov, V., Ladstätter-Weißmayer, Richter, A., Richter, A., DeBeek, R., Hoogen, R., Bramstedt, K., Eichmann, K.-U., Eisinger, M., Perner, D. The global ozone monitoring experiment (GOME): mission concept and first scientific results. *J. Atmos. Sci.* 56, 151–175, 1999.
- Bussemer, M. Der Ring-Effekt: Ursachen und Einfluß auf die spektroskopische Messung stratosphärischer Spurenstoffe. Diplomarbeit, University of Heidelberg, 1993.
- Carn, S.A., Bluth, G.J.S. Prodigious sulfur dioxide emissions from Nyamuragira volcano, D.R. Congo. *Geophys. Res. Lett.* 30 (23), 2211, doi:10.1029/2003GL018465, 2003.
- Carn, S.A., Krueger, A.J., Krotkov, N.A., Gray, M.A. Fire at Iraqi sulfur plant emits SO<sub>2</sub> clouds detected by Earth Probe TOMS. *Geophys. Res. Lett.* 31, L19105, doi:10.1029/2004GL020719, 2004.
- Carn, S.A., Strow, L.L., de Souza-Machado, S., Edmonds, Y., Hannon, S. Quantifying tropospheric volcanic emissions with AIRS: the 2002 eruption of Mt. Etna (Italy). *Geophys. Res. Lett.* 32, L02301, doi:10.1029/2004GL021034, 2005.
- Chance, K., Spurr, R.J.D. Ring effect studies: Rayleigh scattering, including molecular parameters for rotational Raman scattering and the Fraunhofer spectrum. *Appl. Opt.* 36, 5224–5230, 1997.
- Eisinger, M., Burrows, J.P. Tropospheric sulfur dioxide observed by the ERS-2 GOME instrument. *Geophys. Res. Lett.* (25), 4177–4180, 1998.
- Graf, H.-F., Feichter, J., Langmann, B. Volcanic sulfur emissions: estimates of source strength and its contribution to the global sulfate distribution. *J. Geophys. Res.* D102, 10727–10728, 1997.
- Hönninger, G., von Friedeburg, C., Platt, U. Multi axis differential optical absorption spectroscopy (MAX-DOAS). *Atmos. Chem. Phys.* 4, 231–254, 2004.
- Krueger, J. et al. Volcanic sulfur dioxide measurements from the total ozone mapping spectrometer instruments. *J. Geophys. Res.* D100, 14057–14076, 1995.
- Kurucz, R.L., Furenlid, I., Brault, J., Testerman, L. Solar Flux Atlas from 296 to 1300 nm. National Solar Observatory, Sunspot, New Mexico, p. 240, 1984.
- Martin, R.V., Chance, K., Jacob, D.J., Kurosu, T.P., Spurr, R.J.D., Bucseles, E., Gleason, J.F., Palmer, P.I., Bey, I., Fiore, A.M., Li, Q., Yantosca, R.M., Koelemeijer, R.B.A. An improved retrieval of tropospheric nitrogen dioxide from GOME. *J. Geophys. Res.* 107 (D20), 4437, doi:10.1029/2001JD001027, 2002.
- McCormick, M.P., Thomason, L.W., Trepte, C.R. Atmospheric effects of the Mt. Pinatubo eruption. *Nature* 373 (2), 1995.
- NASA Earth Science Missions: Total Ozone Mapping Spectrometer (TOMS)-Earth Probe (EP). Available from: <<http://toms.gsfc.nasa.gov/eptoms/epsat.html>>.
- Perner, D., Platt, U. Detection of nitrous acid in the atmosphere by differential optical absorption. *Geophys. Res. Lett.*, 7, 1979.
- Platt, U. Differential optical absorption spectroscopy (DOAS). in: Air monitoring by spectroscopic techniques *Chem. Anal. Ser.*, 127. Wiley, New York, pp. 27–84, 1994.
- Richter, A., Eisinger, M., Ladstätter-Weißmayer, A., Burrows, J.P. DOAS zenith sky observations. 2. Seasonal variation of BrO over Bremen (53°N) 1994–1995. *J. Atmos. Chem.*, 1998.
- Richter, A., Wagner, T. Diffuser plate spectral structures and their influence on GOME slant columns. Technical note, University of Bremen, January, 2001.
- Richter, A., Burrows, J. Retrieval of tropospheric NO<sub>2</sub> from GOME measurements. *Adv. Space Res.* 29 (11), 1673–1683, 2002.
- Thomas, W., Erbertseder, T., Ruppert, T., van Roozendaal, M., Verdebout, J., Balis, D., Meleti, C., Zerefos, C. On the retrieval of volcanic sulfur dioxide emissions from GOME backscatter measurements. *J. Atm. Chem.* 50, 295–320, doi:10.1007/S10874-005-5079-5, 2005.
- Van Roozendaal, M., Soebijanta, V., Fayt, C., Lambert, J.-C.. Investigation of DOAS issues affecting the accuracy of the GDP version 3.0 total ozone product, in: Lambert, J.-C. (Ed.), ERS-2 GOME GDP 3.0 Implementation and Delta Validation, ERSE-DTEX-EOAD-TN-02-0006, ESA/ESRIN, Frascati, Italy, pp. 97–129, 2002 (Chapter 6).
- von Friedeburg, C., 2003. Derivation of Trace Gas Information combining Differential Optical Absorption Spectroscopy with Radiative Transfer Modelling. PhD Thesis, University of Heidelberg.
- von Glasow, R., Sander, R., Bott, A., Crutzen, P.J. Modeling halogen chemistry in the marine boundary layer 2. Interactions with sulfur and the cloud-covered MBL. *J. Geophys. Res.* 107, 4323, doi:10.1029/2001JD000943, 2002.
- Wagner, T., Leue, C., Pfeilsticker, K., Platt, U. Monitoring of the stratospheric chlorine activation by global ozone monitoring experiment (GOME) OCIO measurements in the austral and boreal winters 1995 through 1999. *J. Geophys. Res.* 106, 4971–4986, 2001a.
- Wagner, T., Leue, C., Wenig, M., et al. Spatial and temporal distribution of enhanced boundary layer BrO concentrations measured by the GOME instrument aboard ERS-2. *J. Geophys. Res.* 106, 24225–24235, 2001b.